Popovich, B., Wotherspoon, L. & Borrero, J. (2021) An assessment of subduction zone-generated tsunami hazards in New Zealand Ports. Nat Hazards 107, 171–193. https://doi.org/10.1007/s11069-021-04578-z

Abstract

For the role they play in domestic and international shipping and inter-island transport, ports are a critical part New Zealand's infrastructure network. With ports located along coastlines having similar exposure to tsunami hazards, multiple facilities could experience structural damage and operational disruption during a single event. In this study we evaluated tsunami effects in terms of water levels and current speeds at 13 ports as caused by both local and distant source subduction zone earthquakes over a range of source moment magnitude scenarios. The results suggest that while the tsunami hazard varies between ports, it is generally highest along the eastern coastline due to its exposure to tsunami generated along the Southern Kermadec, Hikurangi and South American Subduction Zones. While a Hikurangi earthquake has the potential to generate the most devastating impacts at individual ports, an earthquake off the Peruvian coastline has the potential to impact operations and infrastructure at the largest number of ports. Such an event could affect international trade capacity, regional recovery and domestic inter-island transport. Due to the potential for damage and disruption at multiple ports in a single event, this study highlights the importance of a broader national and international transport system perspective to inform potential resilience investments.

1. Introduction

The undeniable destructive capacity of tsunamis was brought to the forefront of global awareness following the 2004 Indian Ocean Tsunami and the 2011 Tohoku Tsunami. Other recent tsunamis have also born largescale impacts including the 2018 Palu Tsunami, 2013 Solomon Islands tsunami, the 2010 and 2015 Chile tsunamis, and the 2009 Samoa tsunami (Okal et al. 2010, Fritz et al. 2011, Aránguiz et al. 2015, Romano et al. 2015, Omira et al. 2019). These events resulted in mass casualties as well as extensive damage to buildings and critical infrastructure. Field surveys conducted in various locations following major tsunami have investigated the impact and damage to buildings (Lukkunaprasit & Ruangrassamee 2008, Reese et al. 2011, Gokon & Koshimura 2012, Fraser et al. 2013) and non-building infrastructure components and networks (Lekkas et al. 2011, Evans & McGhie 2011, Kosa 2012, Akiyama et al. 2013, Zama et al. 2015, Paulik et al. 2019). Port infrastructure has typically been a minor component of field investigations, and in only limited studies were the investigations dedicated largely to their performance (e.g. PIANC 2009, Strand & Masek 2007, Percher et al. 2013, Chua et al. 2020).

Tsunami design loads on buildings and infrastructure have been derived and published in various design standards (FEMA 2011, ASCE 2016, FEMA 2019). Certain components of

tsunami loading are derived from standard fluid mechanics practices (e.g. hydrostatic loading components) whereas other more complex components that pertain specifically to tsunami and port infrastructure are derived from computational and experimental modelling including wave impact (Cuomo et al. 2007, Robertson et al. 2013, Kihara et al. 2015) and vertical uplift (Chen et al. 2016). The available information related to tsunami loading, damage modes, and hazard characteristics has resulted in tsunamis being incorporated into structural design, particularly in the United States (ASCE 2016) and Japan (MLIT 2011a, MLIT 2011b). New Zealand only recently began publishing equivalent guidance documents (MBIE 2020). Loading in these existing standards is related back to the tsunami intensity via either inundation depth or velocity but regardless, their application requires robust deterministic or probabilistic tsunami hazards models.

Numerous tsunami hazard assessments have been conducted for New Zealand both nationally (e.g. Berryman 2005, Power 2013) and for specific sites or regions including Christchurch (Lane et al. 2014), Gisborne (Borrero & Bosserelle 2019), Wellington (Mueller et al. 2015a), and Tauranga (Prasetya & Wang 2011). The Power (2013) study is the most comprehensive national assessment thus far. In that study, probabilistically derived maximum tsunami amplitudes and source disaggregation information are reported for 20-km segments covering the entire New Zealand coastline. However, as with most probabilistic studies, the model results report only a single value for the maximum tsunami amplitude at specific recurrence intervals and do not provide any detail on the water level time series, information critical for detailed hydrodynamic analysis and resolving tsunami induced current speeds. Previous studies on tsunami effects in New Zealand ports include the nationwide overview and hydrodynamic modelling of distant source tsunami at four sites by Borrero et al. (2014), the detailed analysis of Lyttelton Harbour by Borrero and Goring (2015), the broader infrastructure assessment of Auckland (AELG 2014), Turnbull and Hughes (2017) assessment of Port Marlborough and the detailed analysis of tsunami effects at maritime facilities in the Northland Region (including Northport) by Borrero and O'Neill (2019).

This study builds upon these previous assessments by expanding the scope of the inundation modelling in port locations that have been previously examined and providing new assessments focussed specifically on the ports at locations which have either been modelled at a regional or city scale or for which no modelling has been done. Section two of this paper describes the role ports play in New Zealand and provides information on the specific study sites. Section three outlines the methodology including the tsunami hydrodynamic model, the development of the bathymetry, and the details of the seismic source models. Section four summarises the results of each scenario including peak tsunami amplitudes and current speeds, and provides a discussion of the results in the context of each port, as well as implications for the broader national transport system.

2. New Zealand Context

New Zealand is situated along a major plate boundary in the southern Pacific Ocean and as such, is vulnerable to impacts from a wide range of natural hazards including tsunamis. With the majority of the population residing in relatively large coastal cities, many critical infrastructure lifelines are potentially exposed to tsunamis, including ports. Independent researchers and New Zealand's infrastructure lifelines groups have investigated the general impacts from tsunami to New Zealand's lifelines, including ports (AELG 2014, Horspool & Fraser 2016).

While protected river ports have played a role in New Zealand's history, many smaller facilities have closed over the years, leaving most trade to 14 seaports (Figure 1) that facilitate international trade as well as domestic inter and intra-island shipping. These facilities are seen as strategically important through their inclusion as designated lifelines in the Civil Defence and Emergency Management (CDEM) Act of 2002 (NZL 2002), which stipulates that they must be operational to the fullest extent possible following the occurrence of a natural hazard. Due to its small size, lack of international shipping and the relatively low tsunami hazard on the West Coast of New Zealand, Westport Harbour is excluded from this study.

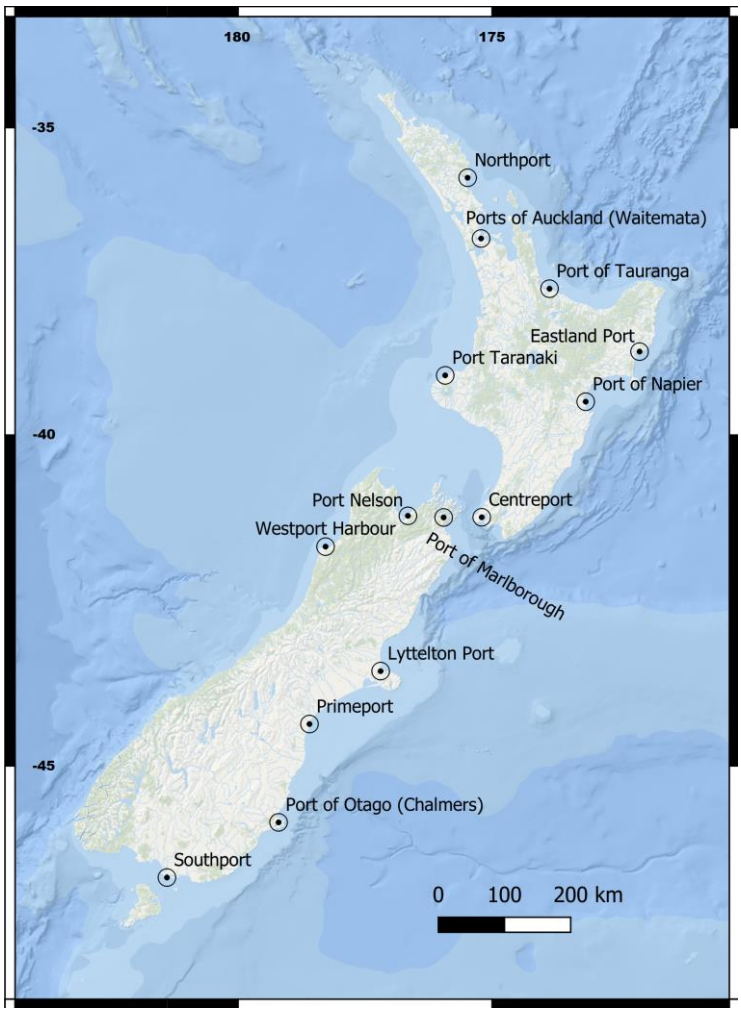

Figure 1: Map of New Zealand with the distribution of seaport locations across the country.

The 13 remaining ports are critical to New Zealand's import/export-based economy. Although the services sector accounts for approximately 2/3 of New Zealand's total gross domestic product (GDP), trade reliant industries account for the bulk of the remainder (The Treasury 2016). Seaports facilitate the vast majority of merchandise imports and exports, in excess of 99% by weight and volume. Figure 2 shows the value of cargo passing through each of New Zealand's main ports for the year 2019 (Statistics NZ 2020). Of note is the large volume of imports moving through the Ports of Auckland, and the large volume of exports moving through the Port of Tauranga. Table 1 provides a summary of the characteristics of each port, including the primary industries and trades that make use of these facilities.

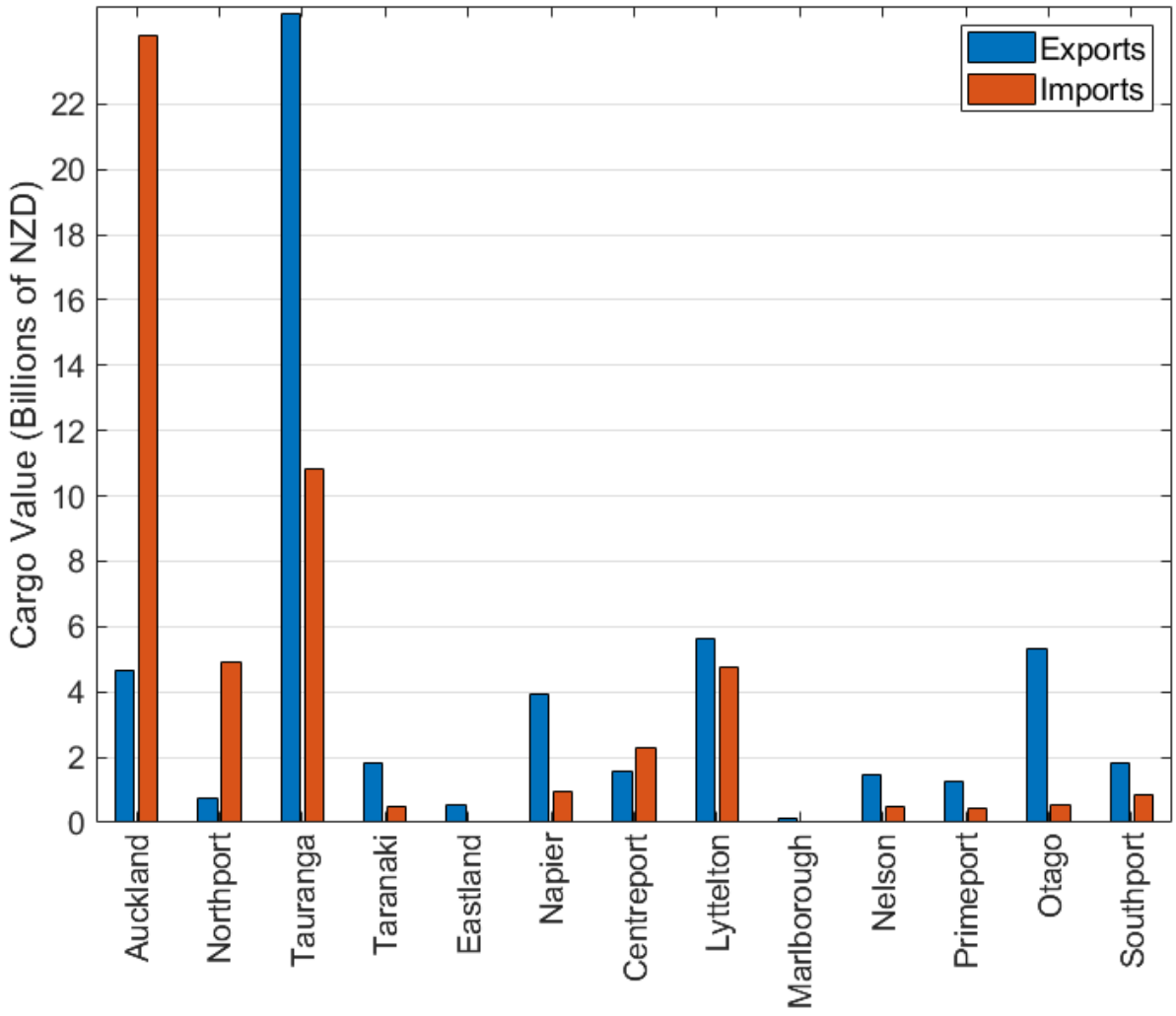

Figure 2: Cargo value of imports and exports passing through New Zealand's major ports. Westport is excluded as it does not facilitate international trade.

Table 1: Names and descriptions of New Zealand's major ports.

Port Name	Description of Facilities and Services
Northport	Deepwater port located on Marsden Point, near Whangarei. Services the Marsden Point Oil Refinery and facilitates forestry exports and imports of gypsum, coal, and fertilizer. Comprises three general purpose berths with a maximum high tide draft of 14.2 metres.
Ports of Auckland	Dominant import seaport in New Zealand featuring the largest container terminal in the country. Facilitates largescale vehicle and machinery imports among numerous other goods. Contains storage for a variety of dry and liquid goods and multiple deepwater berths. Comprises several wharves and berths with a maximum draft of 12.7 metres
Port of Tauranga	New Zealand's largest export port. Primarily services logs, petroleum, cement, agriculture, forestry, and dairy. Comprises large container terminal, bulk dry goods and liquid storage, petroleum storage facilities, a coal yard, cold storage and other facilities. Wharves are located on both the Mount Manganui and Sulphur Point sides of Tauranga Harbour and allow berthing of vessels with up to 14.5 metre drafts.
Port Taranaki	Contains a variety of bulk dry goods and liquids storage facilities. Major shipping facility for petrochemical industry with nearby Taranaki Gas Fields and Methanex (methanol) Plant. Comprises several wharves with a maximum permissible draft of approximately 12.5 metres.
Eastland Port	Small port servicing primarily export of forestry products. Maximum draft of just less than ten metres.
Port of Napier	Medium-sized North Island port servicing mostly forestry exports but also agriculture and other products. Several berths present with a maximum vessel draft of 12.4 metres.
Centreport	North Island point of departure for inter-island ferry services. Contains key fuel terminal, Holcim Cement facilities, and large container terminal. Services a variety imports and exports including forestry and agriculture. Several berths are present with permissible drafts up to 11.3 metres.
Port of Marlborough	Comprises two main wharves. Waimahara which is a deepwater berth facilitating mostly bulk dry goods and forestry exports. Waiotahi is the South Island connection point for inter-island ferries and facilitates a number of cruise ships annually. Maximum permissible ship draft at Waimahara Wharf is approximately 13.5 metres.
Port Nelson	Main goods produced in the region which are exported via Port Nelson include fish, forestry, and apples. Port contains a variety of storage facilities, a small container terminal, and several berths with a maximum allowable draft of 11.3 metres.
Lyttelton Port	Most significant South Island port containing facilities that provide fuel to much of the South Island, a coal yard servicing most west coast coal mines, and the largest South Island container terminal. Facilitates imports and exports including forestry products, gypsum, coal, cement, fish, and agriculture. Max permissible draft along any wharf is 14.5 metres.
Primeport	Comprises facilities to store bulk dry goods, bulk liquids, petroleum, and logs. Primary exports include fish, dairy, forestry, and tallow. Contains several berths with a maximum draft of approximately 11 metres.
Port of Otago	Comprises facilities at two locations: Port Chalmers, and Dunedin. Chalmers is a deepwater port with three berths and a maximum draft of 13.6 metres whereas Dunedin features ten berths with a maximum draft of only 7.9 metres. Key imports and exports include forestry, meat, and dairy. Storage facilities are present for bulk dry goods and liquids as well as a small container terminal.
Southport	Maintains wharf servicing Tiwai Point Aluminium Smelter and Town Wharf servicing mostly petroleum imports. Eight other berths on island harbour range in maximum draft from between seven to 9.7 metres. Hosts Stewart Island Ferry.

3. Methodology

The focus of this study was the assessment of the tsunami hazard from subduction zone earthquakes at New Zealand's 13 largest ports. This consisted of three principal steps, each of which is expanded upon in the following sections. First, a tsunami propagation model was selected through which the local tsunami characteristics were calculated. Second, high-resolution bathymetry models were developed from available topographic and bathymetric data. Finally, tsunami source models were defined as inputs to the tsunami hydrodynamic model.

In this study we considered both local and distant source tsunami. Though tsunamis generated from local crustal earthquakes or submarine landslides also pose a threat to New Zealand ports, the scope of this study was restricted to examining hazard from tsunami generated by subduction zone earthquakes. Source locations include subduction zones most likely to produce the 500 and 2500-year return period tsunami at each port location as per the Power (2013) probabilistic analysis. Inspection of these results reveals that in general, at each site, the same source region is responsible for both the 500 and 2500-year tsunamis with the difference only in the magnitude of the causative earthquake. For local sources, the Hikurangi Subduction Zone presents the most likely source for six ports, the Kermadec Subduction Zone for three ports, and the Puysegur Subduction Zone for three ports. Two source configurations (northern and southern) were used for both the Hikurangi subduction zone and Puysegur subduction zone as shifting the source location can produce a larger tsunami in the ports on different coastlines. For distant sources, the Peruvian section of the South American Subduction Zone (SASZ) presents the most likely source for ten ports while the Chilean segment of the SASZ and the Solomon Islands Subduction Zone each present the most likely source for one port. The key drivers of this research were to assess the relative exposure at each port across these different sources, and to highlight potential scenarios that could be potentially disrupt multiple ports across the national network.

3.1 Tsunami Hydrodynamic Modelling

The numerical modelling presented in this study was performed using the Method Of Splitting Tsunami (MOST) algorithm (Titov and Synolakis 1997, Titov & Gonzalez 1997) and the Community Model Interface for Tsunamis (ComMIT) numerical modeling tool (Titov et al. 2011). The ComMIT model interface was developed by the United States government National Oceanic and Atmospheric Administration's (NOAA) Centre for Tsunami Research (NCTR) following the December 26, 2004 Indian Ocean tsunami as a way to efficiently distribute assessment capabilities amongst tsunami prone countries. The backbone of the ComMIT system is a database of pre-computed deep-water propagation results for tsunamis generated by unit (1 m) displacements on fault plane segments (100 x 50 km) positioned along the world's subduction zones. Using linear superposition, the deep ocean tsunami propagation results from more complex faulting scenarios can be created by scaling and/or combining the pre-computed propagation results from a number of unit sources (Titov et al. 2011). The resulting trans-oceanic tsunami propagation results are then used as boundary inputs for a system of 3 nested near-shore grids covering a coastline of interest. The nested model propagates the tsunami to

the shore computing wave height, velocity, and overland inundation. The use of the ComMIT methodology for accurately modelling both distant and near source tsunami water levels and current speeds in New Zealand ports has been demonstrated in Borrero et al. (2013) and Borrero et al. (2014, 2015a).

3.2 Modelling Grids

Since bathymetry is of first-order importance in the accuracy of hydrodynamic models, new bathymetric grids were developed for each port. Model grids were developed primarily from hydrographic charts from the Land Information New Zealand (LINZ) Data Service (LINZ 2020). While these datasets provided adequate coverage for most of New Zealand, additional digitising was required for each site in areas with sparse coverage. Coastlines were manually digitised as were some offshore depth contours. For some locations, LiDAR data obtained directly from local government agencies supplemented the LINZ datasets. Chart data referenced to lowest astronomical tide (LAT) was converted to mean sea level (MSL) by obtaining average sea level data for MSL and LAT for each port from the tidal levels published in the New Zealand Nautical Almanac 2010-2011 (LINZ 2010).

At each location we constructed a large outer grid at 500 m resolution, an intermediate grid at 150 m resolution and an inner grid immediately surrounding the port at 10 m resolution. As an example, the modelling grids produced for Centerport in Wellington Harbour are shown in Figure 3. The dimensions of the inner grids for each port are listed in Table 2. The grids for Northport and Southport are larger than most others in order to capture the flow of the tsunami through the harbour entrances present at these locations.

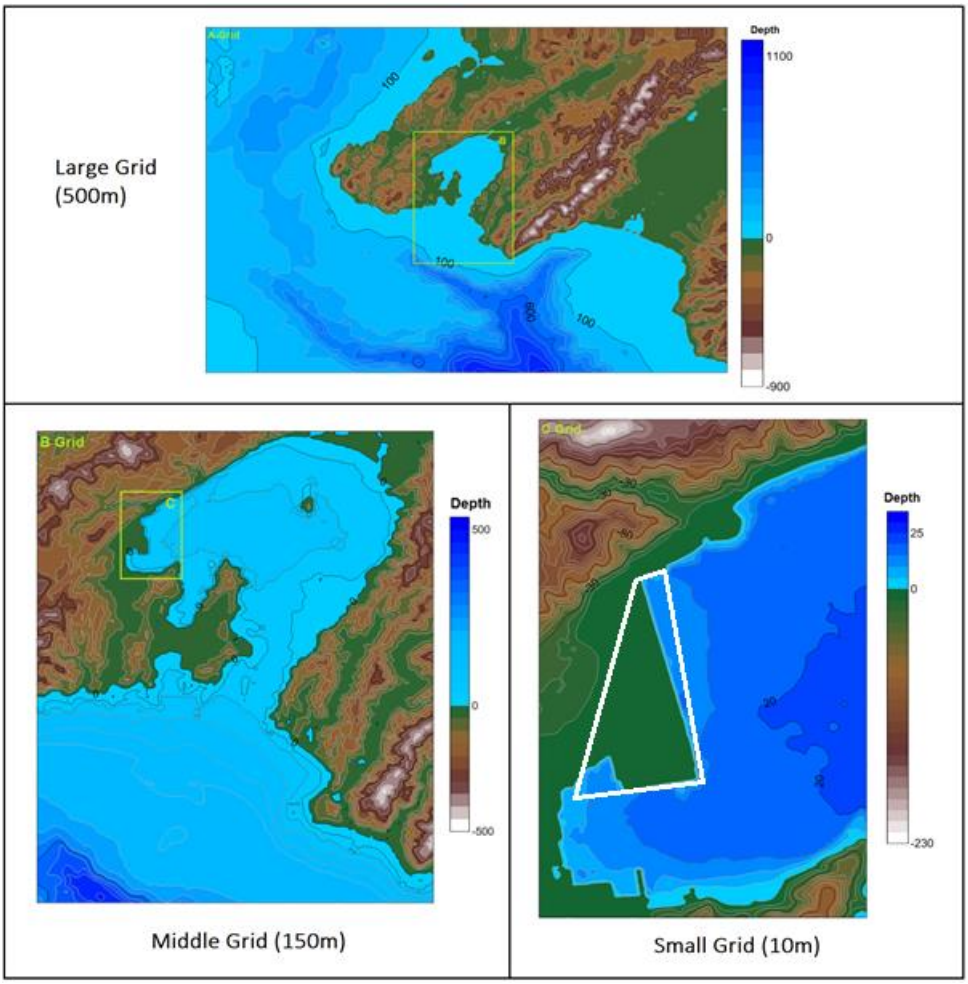

Figure 3: Contour plots generated from each of the three bathymetric grid layers for Centreport in Wellington. Finer grid layers contain substantially more detail. Centreport's position and approximate extents are outlined in white.

Table 2: Dimensions (in nodes) of the innermost,10-m resolution grids covering each port

Port	x-nodes	y-nodes
Northport	679	803
Auckland	479	234
Tauranga	390	869
Taranaki	520	390
Eastland	280	272
Napier	445	286
Centreport	219	442
Marlborough	281	427
Nelson	346	260
Lyttelton	311	304
Primeport	337	445
Otago	194	223
Southport	756	1106

3.3 Tsunami Source Models

As noted above, The ComMIT database stores the full trans-oceanic propagation results (water level *h*, current speed in orthogonal horizontal directions *u* and *v*) for tsunami generated by 1 m slip on individual, 100 km x 50 km fault plane segments positioned along major subduction zones and plate boundaries (see Figure 4 and 5). To define larger or more complicated tsunami sources, the user applies a scaling factor (denoted as α and equivalent to the co-seismic slip in meters) to individual segments and the resultant tsunami wave field is then determined through linear superposition of the results from the individual, scaled solutions. The ComMIT system uses information from global catalogues (i.e. Kirby et al. 2005 as referenced in Gica et al. 2008) to define fault plane geometries in terms of strike, dip and hypocentre depth. The sense of motion for the fault plane rake is assumed to be pure thrust/reverse (i.e. 90 deg.) for segments on the subduction zone interface and pure normal (i.e. -90 deg.) for outer rise type source segments. Using this approach, one may generate an infinite number of unique tsunami sources.

While it is well known that variable slip distribution along the fault plane has a first order effect on the distribution of tsunami heights at the coastline – particularly for near-source events as described by Geist (2002) and demonstrated in New Zealand by Mueller et al., (2015b), this effect is less pronounced for distant source events (Power et al. 2015). Due to the uncertainty associated with modelling variable slip distributions and because we are interested in the relative tsunami exposure across New Zealand ports, we used a uniform slip distribution across the fault plane for this study. Future research could explore the influence of variable slip distributions on resultant tsunami water levels and current speeds.

3.3.1 Earthquake Magnitudes

The upper limit of any fault plane or subduction zone to produce an earthquake is uncertain. The largest earthquake generated by a local New Zealand source in recent history is the 1855 Wairarapa Earthquake which is estimated at M_w 8.2 (Grapes & Downes 1997). There is great uncertainty in the historical record, but studies suggest there is evidence of great ($M_w > 8.0$) earthquakes occurring along local subduction zones, particularly the Hikurangi margin (Clark et al. 2019). The possibility of a whole-margin rupture is also uncertain, but such an event would produce an earthquake of at least M_w 9.0 (Power et al. 2011, Stirling et al. 2012). The South American Subduction Zone, the most likely distant tsunami source for all port locations except Nelson, has produced earthquakes in excess of M_w 9.0 including the event of May 1960, one of the largest earthquakes on record (Kanamori 1977) with magnitude estimates varying from 9.3 to 9.6 (Bilek 2010, Fujii and Satake 2012). Thus, M_w 9.0 and 9.5 for local and distant scenarios respectively are considered justified as upper limits for this modelling. For local source tsunami, seismic source model magnitudes ranged from 7.0 to 9.0 M_w at intervals of 0.5 units. Distant source models were varied from 8.0 to 9.5 M_w at 0.5 intervals.

3.3.2 Tsunami Source Location and Size

As noted above, the tsunami source regions considered for each port were based on the Power (2013) probabilistic study. Source disaggregation results from that study provide guidance on the most likely local or distant source region for each port. Two unique sources were used along the Hikurangi and Puysegur Subduction Zones and a single source for the remainder. Based on this, Centreport, Port Taranaki, and all South Island ports were analysed against a southern Hikurangi source tsunami whereas the remainder were analysed against the northern source configuration on the Hikurangi margin. Southport and all ports on the eastern side of both islands were analysed against the southern Puysegur configuration and all others against the northern. All 13 ports were analysed against the single Kermadec, Chilean, Peruvian, and Solomon Islands sources.

The fault plane dimensions for each of the source scenarios are depicted in Figure 4 and 5 and listed in Table 3. The fault plane areas used for each source conform roughly to scaling relationships of earthquake magnitude and fault plane area indicated by Wells & Coppersmith (1994) and Strasser et al. (2010) with the slip amount determined by the moment magnitude and the assumed fault plane area as per Hanks and Kanamori (1979).

Table 3: Fault plane dimensions and slip amounts (α-values in ComMIT) for each source scenario.

M_w	Fault Plane (km)	Slip (m)
7.0	100x50	0.2
7.5	100x50	1.0
8.0	100x50	5.6
8.5	200x100	7.9
9.0	500x100	17.7
9.5	900x150	36.9

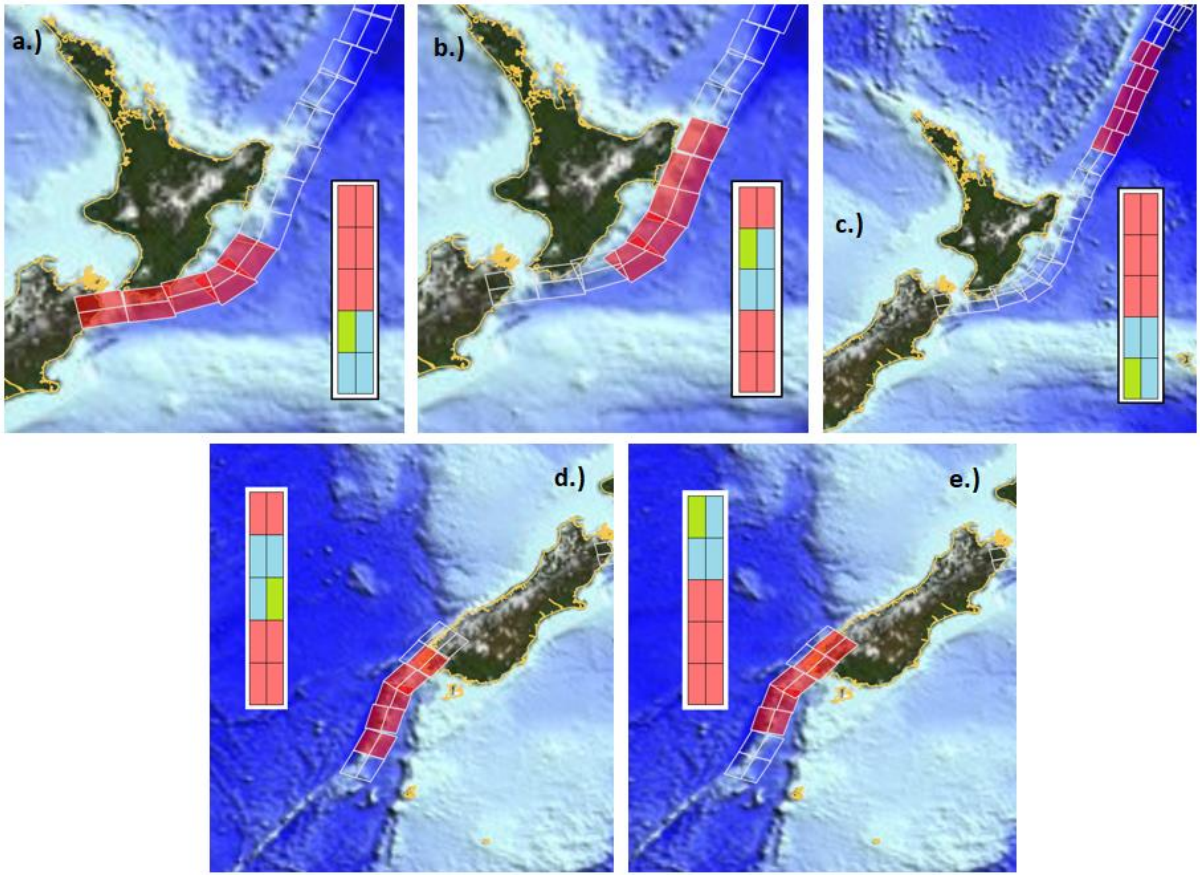

Figure 4: Fault plane segments used for the Hikurangi (a & b), Kermadec (c), and Puysegur (d & e) Subduction Zone tsunami sources. Segment colours indicate those used for the M_w 9.0 (red) M_w 8.5 (blue) and M_w 7.0-8.0 (green) scenarios. Slip amounts applied to each segment are summarised for each magnitude in Table 2. Each rectangle represents a 100x50 km fault segment.

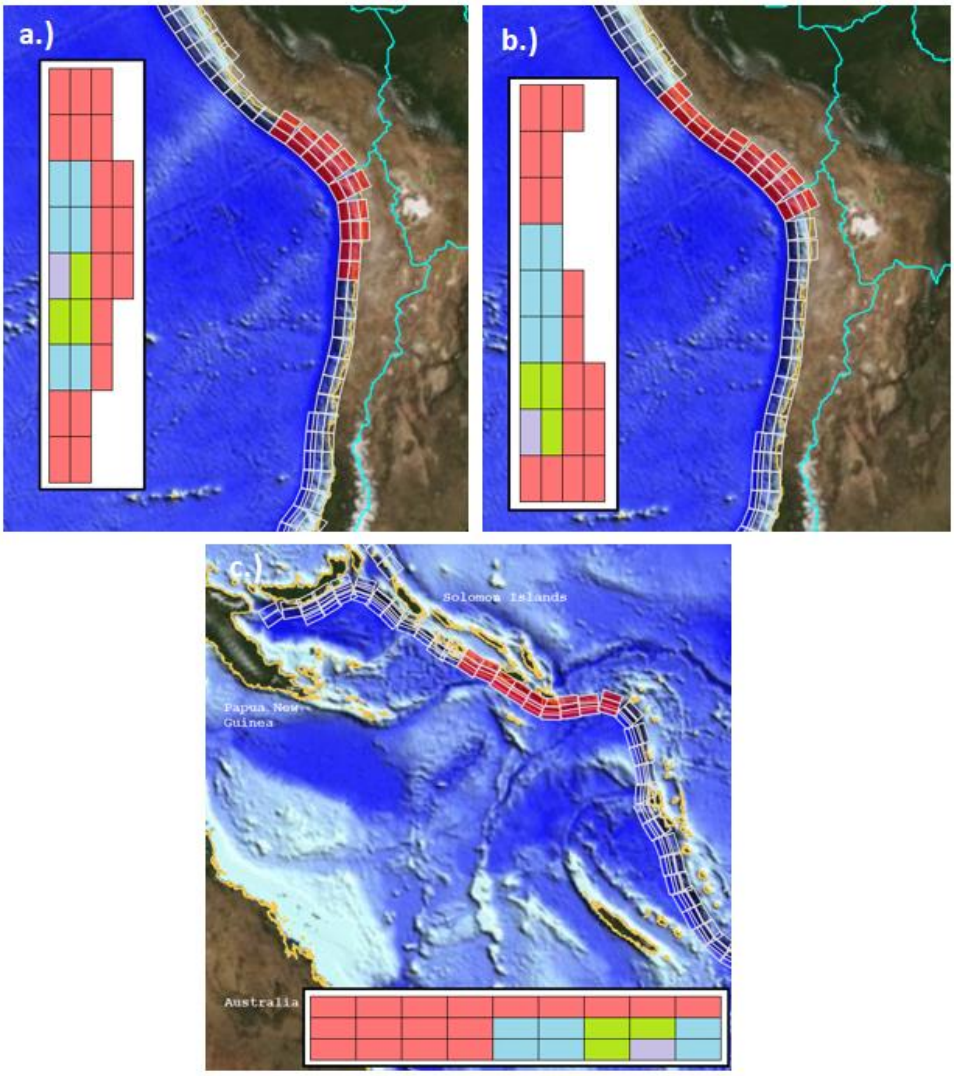

Figure 5: Fault plane segments used for the Chile (a), Peru (b), and Solomon Islands (c) Subduction Zone tsunami sources. Segment colours indicate those used for the M_w 9.5 (red) M_w 9.0 (blue), M_w 8.5 (green) and M_w 8.0 (purple) scenarios. Slip amounts applied to each segment are summarised for each magnitude in Table 2. Each rectangle represents a 100x50 km fault segment.

4. Model Results and Discussion

The ComMIT model was run for each port over each of the source scenarios with the model producing output of tsunami induced water level and current speed over the simulation. In Figure 6 and 7 we plot the maximum computed tsunami water level and current speed from each node in the innermost model grid as a stacked bar plot. This presentation illustrates the variation in maximum water level and current speed as a function of source magnitude with the upper boundary of each section of the stacked bar plot representing the maximum for that source magnitude. The size of each portion of the stacked bar plot shows the increase in the maximum computed amplitude or current speed from one source magnitude to the next. This enables a direct comparison of the maximums for each port and how they compare to other ports across the range of scenarios and source magnitudes. Spurious peaks at isolated nodes in each grid were ignored in the analysis of each scenario as these were interpreted to be numerical artefacts rather than real characteristics.

For tsunami current speeds, we refer to the damage level – current speed relationships defined by Lynett et al. (2014) (Table 4). These relationships are based on damage observations in California ports following both the 2011 Tohoku Tsunami and 2010 Chile tsunami as well as other previously published data that define damage levels as a function of tsunami current speed. In these relationships current speeds below 3 knots are not generally expected to cause damage while current speeds over 9 knots can cause extreme damage to structures and vessels. Using these relationships we can estimate the damage potential from tsunami induced currents at our study sites based on the modelled results. As shown in modelling done by Borrero et al. (2014), tsunami current speeds are much more variable across the model domain than water levels which are more consistent. Lynett et al. (2014) and Borrero et al. (2015b) also show that strong and highly variable currents tend to occur near breakwaters or other impermeable structures or when water flows are constrained, such as when they passing through a narrow channel or around a sharp bend.

Table 4: Current speed damage thresholds defined by Lynett et al. (2014).

Damage	Range of Current Speeds
No damage expected	< 3 knots
Minor/moderate damage possible	Between 3 and 6 knots
Major damage possible	Between 6 and 9 knots
Extreme damage possible	> 9 knots

Among the local scenarios, the Hikurangi sources produce the highest maximum water levels and current speeds and affect the greatest number of ports in a single event. This source region produces potentially destructive effects for ports located on the east coast and the top of the South Island. However, which ports will be most severely affected depends on the source location. Accordingly, the ports of Eastland and Napier see the strongest overall effects with tsunami heights of > 10 m and extreme current speeds (>40 knots) for the M_W 9.0 scenario. In general the ports of Eastland, Napier, Centreport and Lyttelton are most strongly affected with strong but less severe effects at Northport, Tauranga and Marlborough.

The remaining sites see less severe effects. For the M_w 8.5 scenario, the maximum water levels exceed 4 m at three ports (Eastland, Napier and Centreport) with maximum current speeds exceeding 20 knots at Eastland, Napier and Lyttelton. In the M_w 7.5 Hikurangi scenarios, maximum water levels are generally less than 1 m across ports, however maximum modelled current speeds approach the 'major damage' threshold at Eastland and Napier.

The Kermadec sources produce the next largest set of water levels and current speeds, however this source region affects fewer ports simultaneously relative to the Hikurangi sources with the strongest effects confined to ports located on northern and eastern coasts of the North Island. For the M_w 9.0 source, maximum water levels exceed 1.5 m and current speeds exceed 10 knots at Northport, Tauranga, Eastland and Napier. At M_w 8.5, only Northport experiences maximum water levels greater than 1 m, while maximum current speeds exceed the major damage threshold at the same 4 locations noted above. For M_w 7.5 and less, water levels are all less than 50 cm, and currents break the minor/moderate damage range at only Northport and Eastland. In contrast, the Puysegur source scenarios mainly affect ports on the western and southern coasts. Only three ports (Taranaki, Primeport and Southport) experience maximum water levels greater than 1 m for a M_w 9.0 event, with Lyttelton and Southport experiencing maximum current speeds greater than 8 knots.

Among the distant source scenarios, the Peru source produced the highest maximum water levels and current speeds across all ports. For the M_w 9.5 scenario, nine ports had water levels greater than 2 m, with two above 4 m, whereas maximum water levels were less than 2 m across all ports for the M_w 9.0 scenario. In terms of current speed, the M_w 9.5 scenario produced current speeds exceeding 10 knots at 10 ports. The M_w 9.5 Chile source produced current speeds exceeding 10 knots in eight ports with four ports having maximum water levels greater than 2 m, and one above 4 m. At M_w 9.0 two ports experienced a maximum water level greater than 2 m. In contrast, the Solomon Island sources produced mostly insignificant tsunami water levels at all magnitudes other than the M_W 9.5 scenario. However, damaging maximum current speeds were evident for some lower magnitude events.

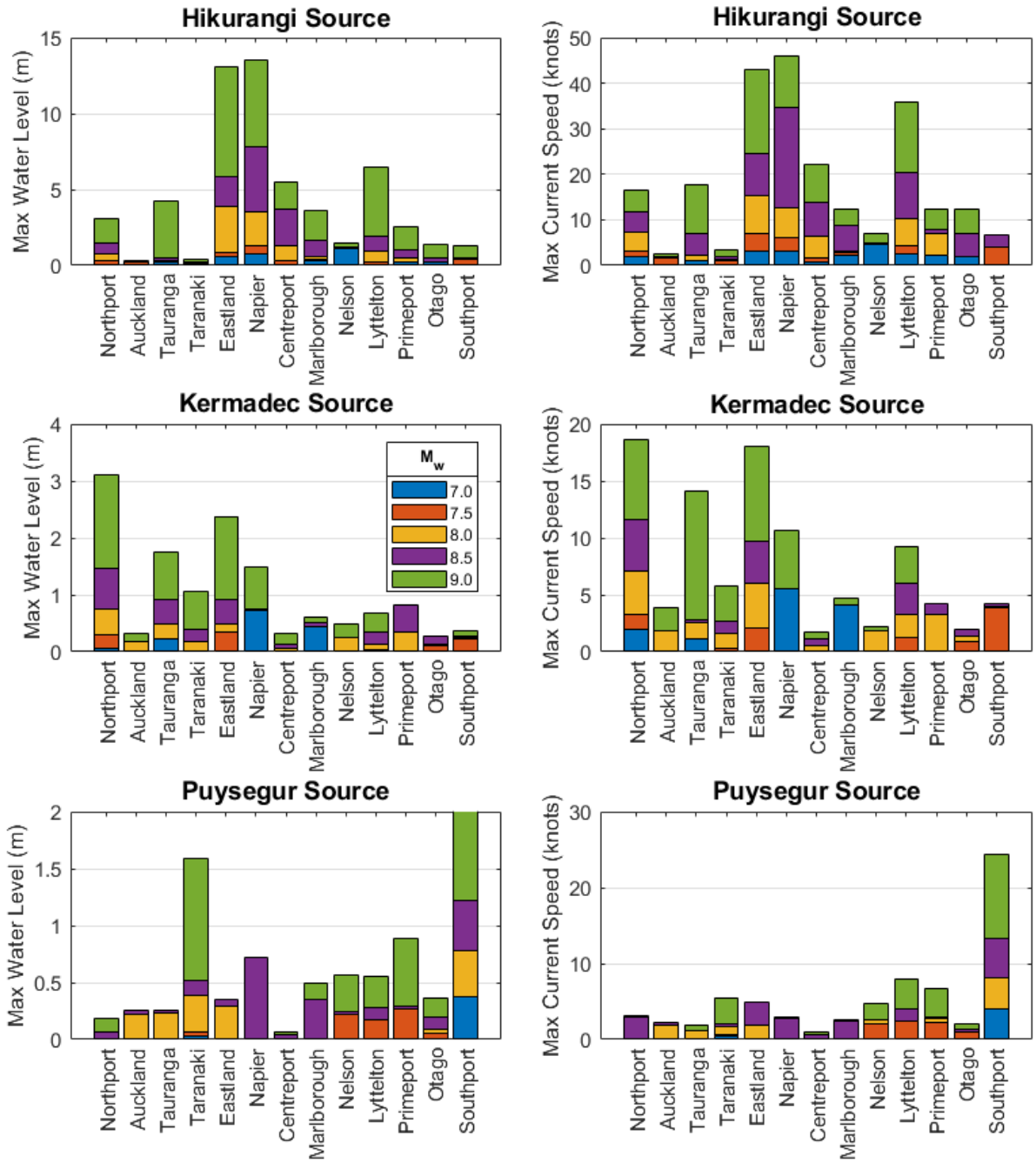

Figure 6: Maximum water levels and current speeds for each port resulting from each local tsunami source model. Results are presented as a stacked bar plot with each tier indicating the cumulative increase in water level and current speed. Note that different vertical scales are used for each source.

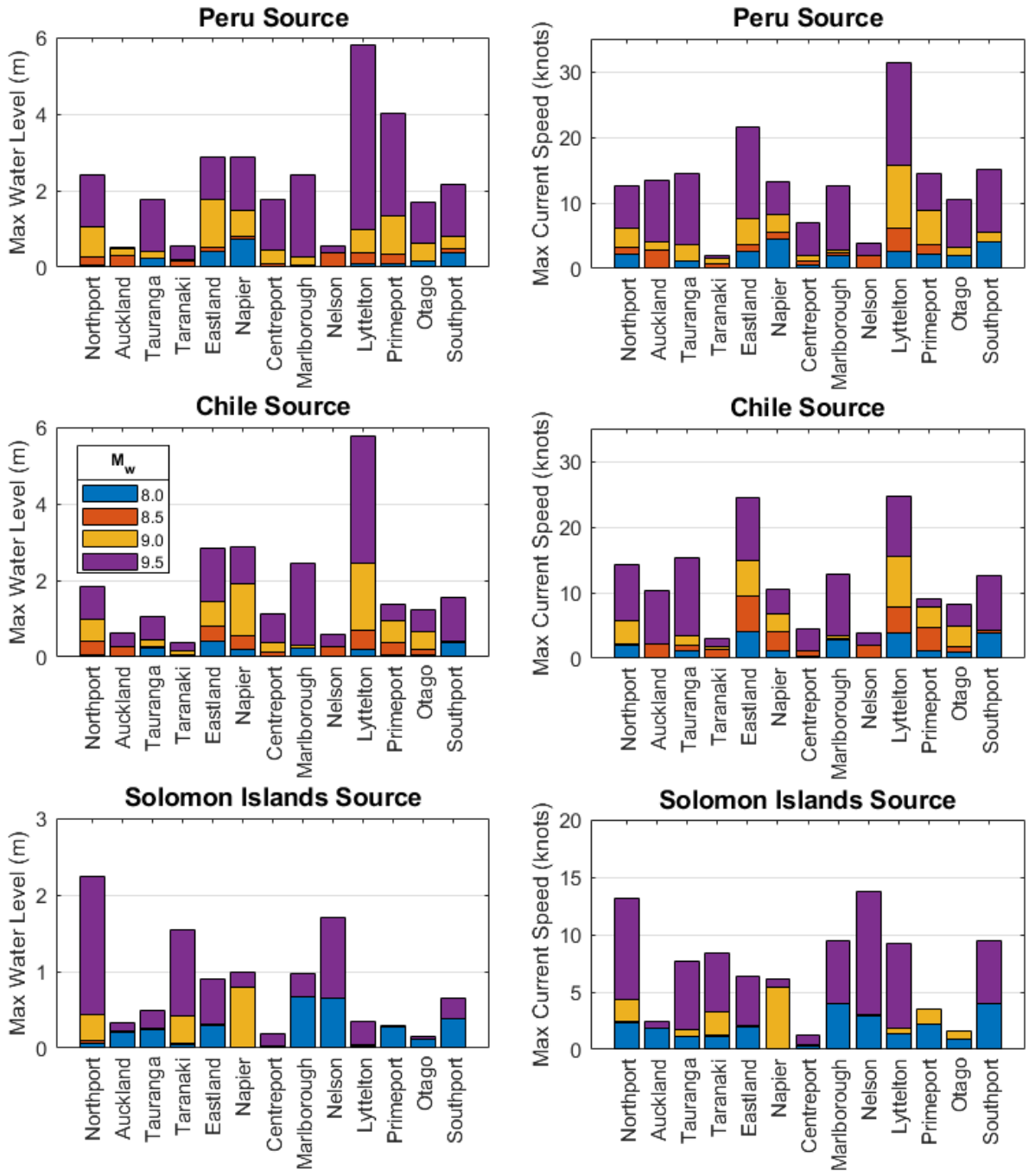

Figure 7: Maximum water levels and current speeds for each port resulting from each unique distant tsunami source model. Results are presented as a stacked bar plot with each tier indicating the cumulative increase in water level and current speed. Note that different vertical scales are used for each source.

4.1 North Island Ports

Local tsunami hazards in Northport are characterised by maximum water levels of over 3 m from M_w 9.0 events from the Kermadec and Hikurangi Subduction Zones. All three distant source subduction zones produce similar tsunami characteristics at Northport with maximum amplitudes around 2 m for M_w 9.5 events. Damaging maximum current speeds are expected for these earthquake magnitudes across all but the Puysegur source events.

Figure 8 presents the spatial variation in maximum water level and current speed for Northport from a M_w 9.0 earthquake on the Kermadec Subduction Zone. Maximum computed water levels are highest along the coast to the south of the port, diminishing into Whangarei Harbour to the north-west. In this situation the water levels at the port would be less damaging, while the higher water levels along the coast could result in damage to refinery infrastructure to the south and east of the port, affecting both onshore and offshore port operations. Maximum current speeds occur within the dredged channel leading up to the port, affecting the shipping channels and the berth locations.

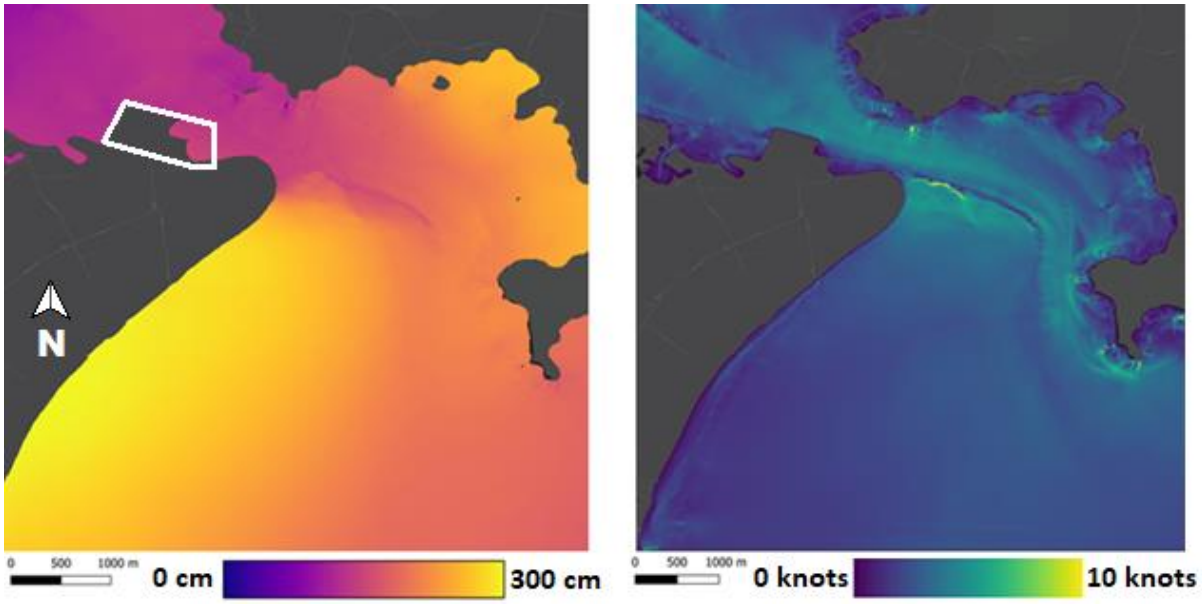

Figure 8: Maximum water level and current speed plots for tsunami at Northport resulting from M_w 9.0 Kermadec Subduction Zone Earthquake. The extent of the port is shown by the white box.

The tsunami hazard at Ports of Auckland is low relative to other sites owing to the protection provided by the shallow waters and complex bathymetry – including numerous islands - of the surrounding Hauraki Gulf as well as the protection afforded by the Coromandel Peninsula to the east. Indeed, the maximum modelled water levels from the M_w 9.5 Chile scenario was less than 1 m and the maximum water level across the near source scenarios was less than 0.5 m, the lowest exposure relative to other ports across the country. However, there is potential for damaging currents to develop in the largest South American source scenarios with maximum current speeds exceeding 10 knots.

The Port of Tauranga, situated within the Tauranga Harbour, has similar exposure trends to those observed at Northport. It is exposed to maximum current speeds in excess of 13 knots

from M_w 9.0 local source tsunami generated along both the Kermadec and Hikurangi Subduction Zones. Northern Hikurangi sources result in maximum water levels greater than 4 m. Distant source tsunami water levels and currents are smaller than local source events. The M_w 9.5 Peru source scenario results in maximum water levels greater than 1.5 m, while M_w 9.5 Chile source scenario produces maximum current speeds of 15 knots.

Eastland Port and Port of Napier lie on the eastern coastline of the North Island in regions predicted to experience some of the largest tsunami in New Zealand (Power 2013). Tsunami amplitudes in both ports were similar through most scenarios and are among the highest analysed in this study. For the northern Hikurangi sources, maximum water levels in both ports exceed 13 m, with local source tsunami from the Kermadec and Puysegur sources significantly smaller. Distant source tsunami generated along the South American Subduction Zone off the coasts of both Peru and Chile result in maximum tsunami amplitudes of just under 3 m in both Eastland Port and Port of Napier for M_w 9.5 events. The setting of Eastland Port within a river mouth result in maximum current speeds greater than those in the open-ocean setting at the Port of Napier for these events, particularly those generated on the Kermadec Subduction Zone.

Centreport is located in Wellington Harbour at the southern end of the North Island and experiences maximum tsunami hazard from local tsunami generated from a southern Hikurangi Subduction Zone source, with maximum water levels greater than 5 m and current speeds exceeding 20 knots for a M_w 9.0 event. The other local source events resulted in insignificant maximum water levels and current speeds. Maximum water levels and current speeds for distant source events were not significant, with only the Peru source resulting in maximum water levels that exceeded 1 m.

Port Taranaki is the sole port in this study located on the western coastline of the North Island. West coast ports experience largest water levels and current speeds from local source tsunami generated along the Puysegur Subduction Zone and distant source tsunami generated along the Solomon Islands. Distant source tsunami generated along the Solomon Islands produce greater tsunami heights and current speeds than those generated along the South American Subduction Zone. In general, local source tsunami produce larger impacts than distant source with all three local source locations producing maximum amplitudes of between 1-2 m, generally less than most other ports.

Figure 9 presents maximum water level and current speed plots for Port Taranaki resulting from a M_w 9.0 earthquake on the Hikurangi Subduction zone. There is a fairly consistent water level of approximately 1.5 m within much of the port boundary, along all major berth locations. These water levels reduce outside the port boundary in the surrounding deeper open waters. The largest current speeds occur near the offshore islands outside the port boundary and off the ends of the breakwaters, cutting across the shipping channel into the port.

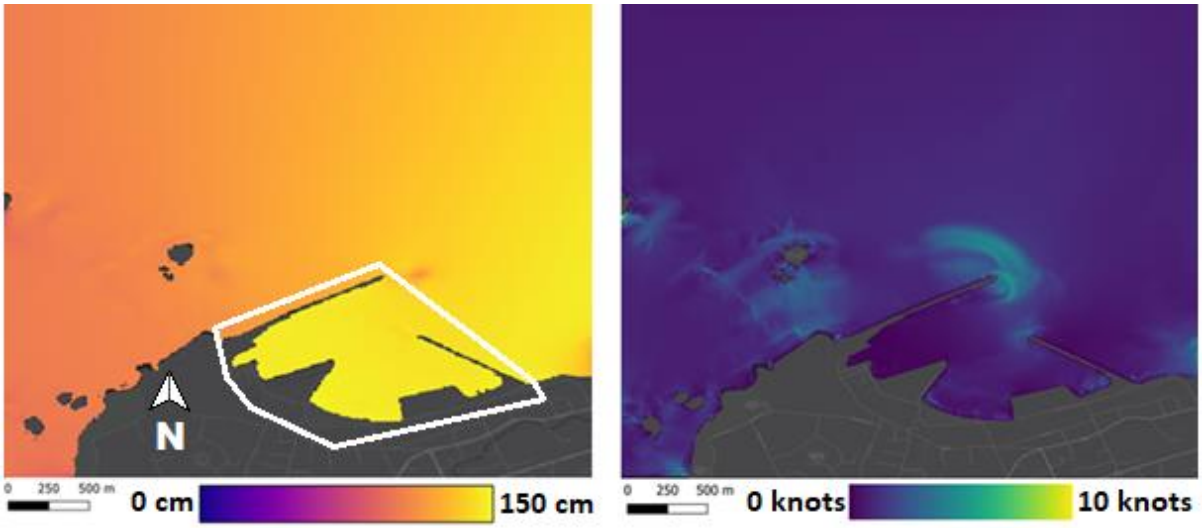

Figure 9: Spatial distribution of maximum water level and current speed for tsunami at Port Taranaki resulting from a M_w 9.0 Hikurangi Subduction Zone Earthquake. The extent of the port is shown by the white box.

4.2 South Island Ports

Port Nelson experiences the greatest distant tsunami hazard from the Solomon Islands-generated events, though the maximum is only 1.7 m. Local source generated water levels are even smaller with the maximum tsunami height generated on the Hikurangi Subduction Zone reaching 1.5 m. Port Nelson experiences maximum tsunami heights of less than 2 m from all six of the sources assessed.

Port Marlborough, also located on the northern end of the South Island, only experiences local source generated water levels greater than 1 m in a from Hikurangi-source events, with maxima exceeding 3 m. Distant source tsunami generated off the Chilean and Peruvian coasts from M_w 9.5 events result in maximum water levels in excess of 2 m, accompanied by inundation of the port and surrounding areas. Similar maximum current speeds are evident for events from both South American Subduction zone sources, exceeding 10 knots for M_w 9.5 events.

Lyttelton Port is the northern-most port on the east coast of the South Island and is situated in Lyttelton Harbour, which is well known for its ubiquitous seiche modes and its tendency to resonate and amplify long wave and tsunami energy (Goring and Henry 1998; Borrero and Goring 2015). Maximum water levels from the M_w 9.0 scenario on the southern Hikurangi margin exceed six metres with current speeds exceeding 30 knots. Lyttelton is also exposed to large maximum water levels from tsunami generated off the Peruvian and Chilean coastlines. In these distant source scenarios, maximum water levels approached six metres and current speeds ranged from 24 to 31 knots – on par with historically observed maxima (c.f. Borrero and Goring, 2014).

Primeport is located in Timaru, south of Lyttelton Harbour on the east coast of the South Island. Maximum tsunami amplitudes from tsunami generated on the southern Hikurangi

margin are smaller than at Lyttelton Port, approximately 2 m for a M_w 9.0 event. Other local sources generate tsunami of less than 1 m at Primeport. Distant source tsunami from a Peru source are particularly well oriented towards Primeport producing maximum water levels of nearly 4 m in the M_w 9.5 scenario.

Port of Otago is located inside the relatively protected Otago Harbour on the southern east coast of the South Island. As such, its tsunami exposure is lower than the other two South Island east coast ports. The largest local source tsunami modelled at Otago is generated from the southern Hikurangi Subduction Zone, with a maximum amplitude of just over 1 m and a current speed of 12 knots for a M_w 9.0 event. Distant tsunami from the Peruvian coastline are able to propagate into the harbour, resulting in maximum water levels of approximately 2 m.

Southport is located near Invercargill on the southern coastline of the South Island. Figure 10 shows water level and current speed for a M_w 9.0 generated tsunami from the Puysegur Subduction Zone at Southport. Maximum water levels are smaller than at many other ports, at only 2.5 m for the M_w 9.0 Puysegur event and 2 m for a distant source M_w 9.5 Peru event. While the water levels are relatively modest, the current speeds are large at this location for both local source and distant source events. For the same Puysegur and Peru scenarios the maximum current speeds are 24 and 15 knots, respectively. As shown in Figure 10, this develops as the tsunami enters the thin entrance channel into Bluff Harbour.

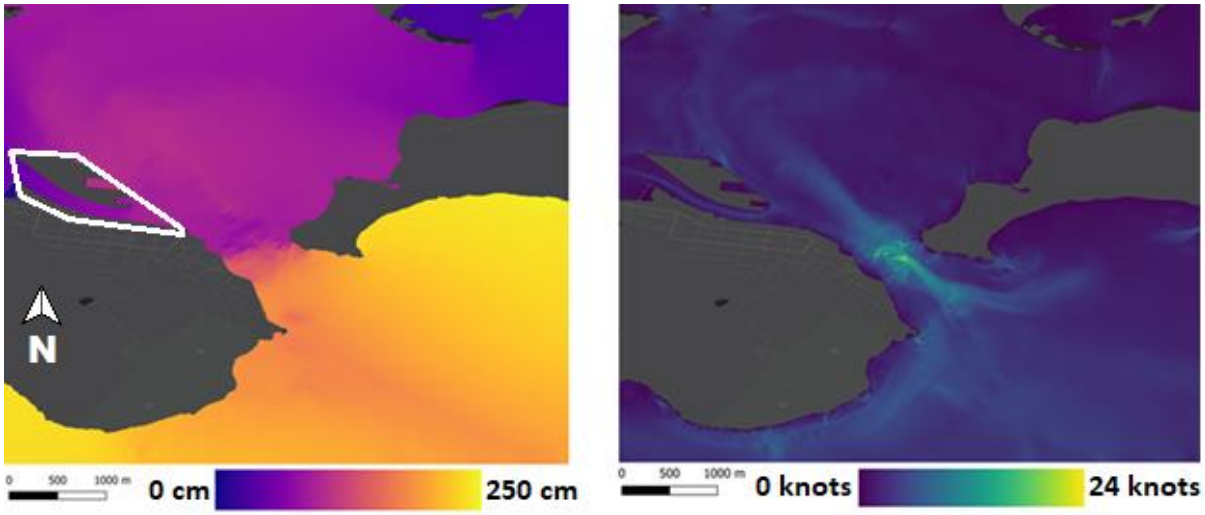

Figure 10: Maximum water level and current speed plots for tsunami at Southport resulting from M_w 9.0 Puysegur Subduction Zone Earthquake. The extent of the port is shown by the white box.

4.3 National Overview

The Port of Auckland has the lowest relative exposure to tsunami hazards in New Zealand. Of the six source regions considered here, none produce highly damaging tsunami amplitudes or current speeds, suggesting that it would most likely be functional after a large tsunami event. This would allow large volumes of imports to continue to enter the country. Similarly, Port of Otago also has relatively low exposure across the tsunami scenarios trialled here and could also be expected to remain functional after a tsunami event.

Port Marlborough and Centreport form a critical pairing of ports, facilitating the inter-island transport link through the Cook Strait between the North and South Islands for road and rail freight. Disruption to either port would have a significant impact on the national transport network. For a M_w 9.0 southern Hikurangi event, maximum water levels of 4 m or greater are evident at both locations and this would likely result in damage or disrupt operations at one or both ports. The other local source events are less likely to impact on these operations, with maximum water levels less than 0.6 m. There could be some damage in distant source Peru events at both locations, with tsunami amplitudes of up to 2 m and currents near 10 knots, beyond the threshold for major damage. For sources from Chile, Centreport would be less impacted, while Port Marlborough would experience wave heights greater than 2 m. Across these sources, strong currents in the Cook Strait could impact on the passage of inter-island shipping for some lower magnitude events.

Though the Hikurangi Subduction Zone produced some of the worst impacts at individual sites, two source configurations were tested and as the Hikurangi margin extends along much of the northeastern coastline, the impact on New Zealand as a whole would depend on where the earthquake occurred. A rupture on the northern end of the Hikurangi margin could produce significant impacts at the Ports of Tauranga, Napier, Northport, and Eastland Port. Impacts at Northport would be a challenge regardless of the other ports affected due to its role servicing the Marsden Refinery. Port of Tauranga is the largest facilitator of exports in New Zealand and services a variety of industries, but the fact that Auckland is not greatly impacted by this scenario could provide an alternative site for freight to be redirected. Port of Napier and Eastland Port both primarily service their respective regions, particularly through export of forestry products and impacts to these ports would be more regionally rather than nationally significant. A tsunami generated on the southern Hikurangi margin would produce lesser impacts on those northern ports, but greater impacts on Centreport, Port of Marlborough, Lyttleton Port, and Primeport. Impacts at Lyttelton Port would be significant as it contains, among other unique infrastructure, fuel facilities that supply most of the South Island. The loss of function of the largest South Island port would be made worse by the potential impacts to the critical linkage between the North and South Islands at Centreport and Marlborough. Primeport is far smaller than the other three ports but is nevertheless regionally significant. Tsunami generated on parts of the Hikurangi margin between what was assessed here or in different slip configurations could generate damaging tsunami at any combination of the ports mentioned here.

Maximum water heights from a M_w 9.0 Kermadec event could disrupt multiple east coast North Island ports. Inter-island transport would still function with Centreport less affected, while export capacity could be severely disrupted due the effects at Tauranga and Napier. Maximum current speeds would affect the functionality of the same ports, along with Lytteton in the South Island. If the magnitude is reduced to M_w 8.5, there is a significant reduction in exposure, with only Northport experiencing maximum water levels greater than 1 m, and only three ports experiencing potentially damaging current speeds.

A large tsunami originating from Peru would present significant challenges for New Zealand. Though the single port maxima do not exceed those of a Hikurangi event in most locations, more ports potentially experience large tsunami. All ports with the exceptions of Nelson and Taranaki could see water levels approaching 2 m, currents exceeding 10 knots, or both. As the 10 knot currents alone are enough to damage port infrastructure, a tsunami from Peru could damage and affect operations at up to ten ports, including all of the largest sites such as Auckland, Tauranga, Lyttelton, and Northport.

Along with the exposure of Port Marlborough for a Chilean source event, Nelson and Lyttelton on the South Island would be significantly impacted, putting pressure on the capacity of cargo handling across the South Island. Maximum current speeds suggest disruption of operations across all ports apart from Centreport. As Lyttelton is the only other port that could support vehicle loading and unloading, the South Island could be left with no facility that could handle the transport of freight vehicles.

5. Conclusions

This study investigated the exposure of New Zealand's seaports to tsunami hazards. This was done through a numerical modelling study using the ComMIT tsunami modelling tool. We developed detailed, high resolution bathymetry models for New Zealand's 13 major ports and identified the most likely source regions to produce a damaging tsunami along New Zealand's coast. Sources were modelled across a range of magnitudes and the model results analysed to provide a generalised assessment of the relative tsunami exposure across New Zealand's port network.

East Coast ports proved to be the most exposed to tsunami hazards, particularly those on the North Island, due to their proximity to and orientation towards the Hikurangi and the South American Subduction Zones. Most ports are exposed to large tsunami and strong currents from a smaller number of subduction zone sources, while Ports of Auckland is not significantly exposed to any of the sources investigated. For individual events, those generated along the Hikurangi Subduction Zone and the South American Subduction Zone would have the most severe impact on New Zealand's ports. A M_w 9.0 earthquake on the Hikurangi Subduction Zone could produce tsunami heights of over 4 m in up to five ports and currents of over 20 knots in up to four ports depending on the source configuration. Though tsunami sources in Peru and Chile produced similar effects, consequences from the Peruvian

sources were somewhat more severe, producing maximum tsunami heights of over 2 m in nine ports and current speeds in excess of 10 knots in ten ports. A number of scenarios could result in damage and disruption across multiple ports, affecting import and export, regional recovery, and inter-island freight and travel. These broader impacts highlight the importance of assessing ports as key linked components of the national transport system, in order to explore system level options to improve resilience and redundancy.

6. Acknowledgements

We acknowledge the funding from the University of Auckland and the Resilience to Nature's Challenges National Science Challenge.

References

AELG. (2014). Auckland Engineering Lifelines Project, Stage 2: Assessing Auckland's Infrastructure Vulnerability to Natural and Man-Made Hazards and Developing Measures to Reduce Our Region's Vulnerability. Auckland, New Zealand: Auckland Engineering Lifelines Group.

Akiyama, M., Frangopol, D., Arai, M., & Koshimura, S. (2013). Reliability of Bridges Under Tsunami Hazards: Emphasis on the 2011Tohoku-Oki Earthquake. *Earthquake Spectra*, 29(1S), p. S295-S314.

Aránguiz, R., González, G., González, J., Catalán, P., Cienfuegos, R., Yagi, Y., Okuwaki, R., Urra, L., Contreras, K., Del Rio, I., & Rojas, C. (2015). The 16 September 2015 Chile Tsunami from the Post-Tsunami Survey and Numerical I Perspectives. *Pure and Applied Geophysics*, 173(2), p. 333-348.

ASCE. (2016). Minimum Design Loads and Associated Criteria for Buildings and Other Structures. Reston, Virginia, USA: American Society of Civil Engineers.

Berryman, K. (2005). Review of Tsunami Hazard and Risk in New Zealand. Lower Hutt, New Zealand: Institute of Geological and Nuclear Sciences.

Bilek, S. L. (2010). Seismicity along the South American subduction zone: Review of large earthquakes, tsunamis, and subduction zone complexity. *Tectonophysics*, 495(1–2), 2–14. doi:10.1016/j.tecto.2009.02.037.

Borrero, J., Bell, R., Csato, C., DeLange, W., Greer, D., Goring, D., Pickett, V. and Power, W. (2013). Observations, Effects and Real Time Assessment of the March 11, 2011 Tohoku-oki Tsunami in New Zealand. *Pure and Applied Geophysics*, 170, 1229-1248, DOI 10.1007/s00024-012-0492-6

Borrero, J., Goring, D., Greer, S., & Power, W. (2014). Far-Field Tsunami Hazard in New Zealand Ports. *Pure and Applied Geophysics*, 172, p. 731-756.

Borrero, J., & Goring, D. (2015). South American Tsunamis in Lyttelton Harbour, New Zealand. *Pure and Applied Geophysics*, 172, p. 757-772.

Borrero, J. C., LeVeque, R. J., Greer, S. D., O'Neill, S. and Davis, B. N. (2015a). Observations and Modelling of Tsunami Currents at the Port of Tauranga, New Zealand, Proceedings of Coasts and Ports Conference, Auckland, New Zealand, September, 2015.

Borrero, J. C., Lynett, P.J. and Kalligeris, N. (2015b). Tsunami Currents in Ports, *Philosophical Transactions of the Royal Society A*. 373: 20140372. http://dx.doi.org/10.1098/rsta.2014.0372

Borrero, J. & Bosserelle, C. (2019). Tsunami Inundation Assessment for the Gisborne District Council. eCoast Ltd. Technical report prepared for the Gisborne District Council.

Borrero, J. and O'Neill. (2019). Development of Products and Procedures for the Mitigation of Tsunami Hazards at Maritime Facilities in Northland, report prepared for the National Emergency Management Agency Resilience Fund, July 2019. https://www.civildefence.govt.nz/assets/Uploads/CDEM-Resilience-Fund/2018-19/2018-08-01-Northland-Maritime-V4.pdf

Chen, C., Melville, B., Nandasena, N., Shamseldin, A., & Wotherspoon, L. (2016). Experimental Study of Uplift Loads Due to Tsunami Bore Impact on a Wharf Model. *Coastal Engineering*, 117, p. 126-137.

Chua, C. T., Switzer, A. D., Suppasri, A., Li, L., Pakoksung, K., Lallemant, D., Jenkins, S. F., Charvet, I., Chua, T., Cheong, A., and Winspear, N. (2020). Tsunami damage to ports: Cataloguing damage to create fragility functions from the 2011 Tohoku event. *Nat. Hazards Earth Syst. Sci.* Discuss. [preprint], https://doi.org/10.5194/nhess-2020-355, in review, 2020.

Clark, K., Howarth, J., Litchfield, N., Cochran, U., Turnbull, J., Dowling, L., Howell, A., Berryman, K., & Wolfe, F. (2019). Geological Evidence for Past Large Earthquakes and Tsunamis Along the Hikurangi Subduction Margin, New Zealand. *Marine Geology*, 412, p. 139-172.

Cuomo, G., Tirindelli, M., Allsop, W. (2007). Wave-in-deck loads on exposed jetties. *Coastal Engineering*, 54(9), p. 657-679. doi:10.1016/j.coastaleng.2007.01.010.

Evans, N. & McGhie, C. (2011). The Performance of Lifeline Utilities Following the 27th February 2010 Maule Earthquake Chile. *9th Pacific Conference on Earthquake Engineering*, Auckland, New Zealand.

FEMA. (2011). Coastal Construction Manual, 4th Edition. FEMA Report P-55. Federal Emergency Management Agency.

FEMA. (2019). Guidelines for the Design of Structures for Vertical Evacuation from Tsunamis, 3rd Edition. FEMA Report P-646. Federal Emergency Management Agency.

Fraser, S., Raby, A., Pomonis, A., Goda, K., Chian, S.C., Macabuag, J., Offord, M., Saito, K. and Sammonds, P. (2013). Tsunami damage to coastal defences and buildings in the March 11th 2011 Mw 9.0 Great East Japan earthquake and tsunami. *Bulletin of Earthquake Engineering*, 11, p. 205-239.

Fritz, H., Petroff, C., Catalan, P., Cienfuegos, R., Winckler, P., Kalligeris, N., Weiss, R., Barrientos, S., Meneses, G., Valderas-Bermejo, C., Ebeling, C., Papadopoulos, A., Contreras, M., Almar, R., Dominguez, J., & Synolakis, C. (2011). Field Survey of the 27 February 2010 Chile Tsunami. *Pure and Applied Geophysics,* 168, p. 1989-2010.

Fujii, Y. & Satake, K. (2012). Slip Distribution and Seismic Moment of the 2010 and 1960 Chilean Earthquakes Inferred From Tsunami Waveforms and Coastal Geodetic Data. *Pure and Applied Geophysics*, 170, p. 1493-1509.

Geist, E. (2002). Complex Earthquake Rupture and Local Tsunamis. *Journal of Geophysical Research B: Solid Earth*, 107(5), p. 2086-2091.

Gica, E., Spillane, M., Titov, V.V., Chamberlin, C.D., and Newman, J.C. (2008), Development of the forecast propagation database for NOAA's Short-term Inundation Forecast for Tsunamis (SIFT), NOAA Tech. Memo. OAR PMEL-139, NTIS: PB2008-109391, 89 pp.

Gokon, H. & Koshimura, S. (2012). Mapping of Building Damage of the 2011 Tohoku Earthquake Tsunami in Miyagi Prefecture. *Coastal Engineering Journal*, 54(1), p. 1250006/1-125006/12.

Goring, D., and Henry, R. (1998). Short period (1–4 h) sea level fluctuations on the Canterbury coast, N. Z. *J. Mar. Fresh*. 32, 119–134.

Grapes, R., and G. Downes. (1997). The 1855 Wairarapa, New Zealand, earthquake: Analysis of historical data. *Bull. N. Z. Soc. Earthquake Eng*., 30(4), 271–368.

Hanks, T., & Kanamori, H. (1979). A Moment Magnitude Scale. *Journal of Geophysical Research*, *84*(B5), 2348–2350.

Horspool, N., & Fraser, S. (2016). An Analysis of Tsunami Impacts to Lifelines, GNS Science Report 2016/22. Lower Hutt, New Zealand: Institute of Geological and Nuclear Sciences.

Kanamori, H. (1977). The Energy Release in Great Earthquakes. *J. Geophys. Res*., 82(20), 2981–2987.

Kihara, N., Niida, Y., Takabatake, D., Kaida, H., Shibayama, A. and Miyagawa, Y. (2015). Large-scale experiments on tsunami induced pressure on a vertical tide wall. *Coastal engineering*, 99, p. 46-63, https://doi.org/10.1016/j.coastaleng.2015.02.009.

Kosa, K. (2012). Damage Analysis of Bridges Affected by Tsunami Due to the Great East Japan Earthquake. *International Symposium on Engineering Lessons Learned from the 2011 Great East Japan Earthquake*, p. 1386-1397.

Kirby, S., Geist, E., Lee, W. H. K., Scholl, D., and Blakely, R. (2005). Tsunami source characterization for Western Pacific subduction zone: A preliminary report. USGS Tsunami Subduction Zone Working Group, USGS White paper.

Lane, E., Kohout, A., Chiaverini, A., & Arnold. J. (2014). Updated Inundation Modelling in Canterbury from a South American Tsunami. NIWA Client Report CHC2014-100. Christchurch, New Zealand: National Institute of Water and Atmospheric Research.

Lekkas, E., Andreadakis, E., Alexoudi, V., Kapourani, E., & Kostaki, I. (2011). The Mw=9.0 Tohoku Japan Earthquake (March 11, 2011) Tsunami Impact on Structures and Infrastructure. *Environmental Geosciences and Engineering Survey for Territory Protection and Population Safety (EngeoPro-2011)*, p. 97-103.

LINZ. (2010). New Zealand Nautical Almanac: 2010/11 Edition. Wellington, New Zealand: Land Information New Zealand.

LINZ. (2020). LINZ Data Service. Wellington, New Zealand: Land Information New Zealand. https://data.linz.govt.nz/

Lukkunaprasit, P. & Ruangrassamee, A. (2008). Building Damage in Thailand in the 2004 Indian Ocean Tsunami and Clues for Tsunami Resistant Design. *The IES Journal Part A: Civil & Structural Engineering*, *1*(1), 17-30.

Lynett, P., Borrero, J., Son, S., Wilson, R., and Miller, K. (2014). Assessment of the Tsunami-Induced Current Hazard. *Geophysical Research Letters*, 41(6), p. 2048-2055.

MBIE. (2020). Tsunami Loads and Effects on Vertical Evacuation Structure: Technical Information. Ministry of Business, Innovation, and Enterprise.

MLIT. (2011a). Concerning Setting the Safe Structure Method for Tsunamis Which are Presumed When Tsunami Inundation Occurs – Note 1318. Tokyo, Japan: Ministry of Land, Infrastructure, Transport, and Tourism.

MLIT. (2011b). Further Information Concerning the Design Method of Safe Buildings that are Structurally Resilient to Tsunami. Tokyo, Japan: Ministry of Land, Infrastructure, Transport, and Tourism.

Mueller, C., Power, W., & Wang, X. (2015a). Hydrodynamic Inundation Modelling and Delineation of Tsunami Evacuation Zones for Wellington Harbour. GNS Science Consultancy Report 2015/176. Lower Hutt, New Zealand: Geological and Nuclear Sciences.

Mueller, C., Power, W., Fraser, S., & Wang, X. (2015b). Effects of Rupture Complexity On Local Tsunami Inundation: Implications for Probabilistic Tsunami Hazard Assessment By Example. *Journal of Geophysical Research: Solid Earth*, 120, p. 488-502.

NZL. (2002). Public Act 2002 No. 33: Civil Defence Emergency Management Act 2002. New Zealand Legislation. From http://www.legislation.govt.nz/act/public/2002/0033/latest/DLM149789.html

Okal, E., Fritz, H., Synolakis, C., Borrero, J., Weiss, R., Lynett, P., Titov, V., Foteinis, S., Jaffe, B., Liu, P., & Chan, I. (2010). Field Survey of the Samoa Tsunami of 29 September 2009. *Seismological Research Letters*, 81(4), p. 577-591.

Omira, R., Dogan, G., Hidayat, R., Husrin, S., Prasetya, G., Annunziato, A., Proietti, C., Probst, P., Paparo, M., Wronna, M., Zaytsev, A., Pronin, P., Giniyatullin, A., Putra, P., Hartanto, D., Ginanjar, G., Kongko, W., Pelinovsky, E., & Yalciner, A. (2019). The September 28th, 2018, Tsunami in Palu-Sulawesi, Indonesia: A Post-Event Field Survey. *Pure and Applied Geophysics*, p. 1-17.

Paulik, R., Gusman, A., Williams, J.H., Pratama, G.M., Lin, S.L., Prawirabhakti, A., Sulendra, K., Zachari, M.Y., Fortuna, Z.E.D., Layuk, N.B.P. and Suwarni, N.W.I. (2019). Tsunami hazard and built environment damage observations from Palu City after the September 28 2018 Sulawesi earthquake and tsunami. *Pure and Applied Geophysics*, 176, p. 3305-3321, https://doi.org/10.1007/s00024-019-02254-9.

PIANC. (2009). Mitigation of Tsunami Disasters in Ports. PIANC Technical Report. World Association for Waterborne Transport Infrastructure.

Percher, M. Bruin, W., Dickenson, S. and Eskijian, M. (2013). Performance of port and harbor structures impacted by the March 11, 2011 Great Tohoku Earthquake and Tsunami. *Ports 2013: Success Through Diversification*, p. 610-619, http://doi/10.1061/9780784413067.063.

Power, W. L., Wallace, L., Wang, X., & Reyners, M. (2011). Tsunami Hazard Posed to New Zealand by the Kermadec and Southern New Hebrides Subduction Margins: An Assessment Based on Plate Boundary Kinematics, Interseismic Coupling, and Historical Seismicity. *Pure and Applied Geophysics, 169*(1–2), 1–36. https://doi.org/10.1007/s00024-011-0299-x

Power, W. L. (compiler). 2013. Review of Tsunami Hazard in New Zealand (2013 Update), GNS Science Consultancy Report 2013/131. 222 p.

Power, W., Borrero, J., Greer, D. and Goring, D. (2015) Developing robust tsunami forecasts for Ports and Harbours, Proceedings of Coasts and Ports Conference, Auckland, New Zealand, September, 2015.

Prasetya, G. & Wang, X. (2011). Tsunami Inundation Modelling for Tauranga and Mount Manganui. GNS Science Consultancy Report 2011/193. Lower Hutt, New Zealand: Geological and Nuclear Sciences.

Reese, S., Bradley, B.A., Bind, J., Smart, G., Power, W. and Sturman, J. (2011). Empirical building fragilities from observed damage in the 2009 South Pacific tsunami. *Earth-Science Reviews*, 107, p. 156-173, https://doi.org/10.1016/j.earscirev.2011.01.009.

Robertson, I., Paczkowiski, K, Riggs, H., & Mohamed, A. (2013). Experimental Investigation of Tsunami Bore Forces on Vertical Walls. *Journal of Offshore Mechanics and Arctic Engineering*, 135(2).

Romano, F., Molinari, I., Lorito, S., & Piatanesi, A. (2015). Source of the 6 February 2013 M_w=8.0 Santa Cruz Islands Tsunami. *Natural Hazards and Earth System Sciences*, 15, p. 1371-1379.

Statistics NZ. (2020). Infoshare: Statistics New Zealand. from http://www.stats.govt.nz/infoshare/

Stirling, M., McVerry, G., Gerstenberger, M., Litchfield, N., Van Dissen, R., Berryman, K., Barnes, P., Wallace, L., Villamor, P., Langridge, R., Lamarche, G., Nodder, S., Reyners, M., Bradley, B., Rhoades, D., Smith, W., Nicol, A., Pettinga, J., Clark, K., & Jacobs, K. (2012). National Seismic Hazard Model for New Zealand: 2010 Update. *Bulletin of the Seismological Society of America*. 102(4), p. 1514-1542.

Strand, C., & Masek, J. (2007). Seaports and Harbors. *Sumatra-Andaman Island Earthquake and Tsunami of December 26, 2004: Lifeline Performance*. Reston, Virginia: American Society of Civil Engineers.

Strasser, F. O., Arango, M. C., & Bommer, J. J. (2010). Scaling of the Source Dimensions of Interface with Moment Magnitude. *Seismological Research Letters*, *81*(6), 941–950. https://doi.org/10.1785/gssrl

Titov, V. & Gonzalez, F. (1997). Implementation and Testing of the Method of Splitting Tsunami (MOST) Model. *NOAA Report No. ERL PMEL-112*.

Titov, V. & Synolakis, C. (1997). Extreme Inundation Flows During the Hokkaido-Nansei-Oki Tsunami. *Geophysical Research Letters*, 24(11), p. 1315-1318.

Titov, V., Moore, C., Greenslade, D., Pattiaratchi, C., Badal, R., Synolakis, C., & Kanoglu, U. (2011). A New Tool for Inundation Modeling: COMmunity Modeling Interface for Tsunamis (ComMIT). *Pure and Applied Geophysics*, 168, p. 2121-2131.

The Treasury. (2016). New Zealand Economic and Financial Overview 2016. Report from The Treasury of New Zealand.

Turnbull, J. and Hughes, M., (2017) Anticipation Tsunami Impacts in Port Marlborough, University of Canterbury Research Report 2017-04, ISSN 1172-9511.

Wells, D., & Coppersmith, K. (1994). New Empirical Relationships among Magnitude, Rupture Length, Rupture Width, Rupture Area, and Surface Displacement. *Bulletin of the Seismological Society of America*, *84*(4), 974–1002.

Zama, S., Nishi, H., Hatayama, K., Yamada, M., Yochihara, H., & Ogawa Y. (2015). On Damage of Oil Storage Tanks Due to the 2011 Off the Pacific Coast of Tohoku Earthquake (M_w 9.0) Japan. *World Conference on Earthquake Engineering 2015*, Lisbon, Portugal.